Journal of
Ceramic Science
and Technology

J. Ceram. Sci. Technol., **08** [4] 493-498 (2017)
DOI: 10.4416/JCST2017-00027
available online at: http://www.ceramic-science.com

The Interaction of Stacking Faults and the Doping of Si in TiC

Q. Liu*, F.G. Qi, X.L. Wang, H.M. Ding, Y. Shi

School of Energy Power and Mechanical Engineering, North China
Electric Power University, Baoding 071003, PR China

received April 26, 2017; received in revised form May 21, 2017; accepted June 2, 2017

Abstract

In this work, the interaction of stacking faults and the doping of Si in TiC has been studied. It has been found that the SFs and doping of Si influence each other, but the effect is limited. However, both of them are closely related to the carbon vacancies. It is considered that the carbon vacancies simultaneously promote the formation of SFs and the doping of Si, and then the doped Si and carbon vacancies tend to segregate in the SF layers, which can result in the formation of Ti_3SiC_2 platelets. And the segregation process can be enhanced by their easier diffusion in the SF layers.

Keywords: Defects, ceramic, vacancies, simulation.

I. Introduction

TiC has been widely used in many fields owing to its high hardness, high-temperature stability and low density [1–3]. However, like other ceramic materials, its ductility is a disadvantage. Therefore, methods to improve its ductility would be very useful for its application, especially in ceramic composites.

It has been found that Si/Al can be doped in TiC, which results in the formation of structurally related Ti_3SiC_2/Ti_3AlC_2 platelets [4,5]. It is known that Ti_3SiC_2/Ti_3AlC_2 belongs to the so-called $M_{n+1}AX_n$ phase (where M is an early transition metal, A is an A-group element and X is carbon and/or nitrogen). Compounds of this family contain two alternately stacked fundamental structural units: the non-stoichiometric transition metal carbide or nitride slabs in NaCl-type crystal structure and the close-packed A-group atomic plane [6]. Owing to this structural characteristic, $M_{n+1}AX_n$ compounds exhibit unusual combinations of properties of carbide/nitride and metal [6,7]. Therefore, it is considered that the *in-situ* formation of the Ti_3SiC_2/Ti_3AlC_2 platelets in TiC crystal would be a promising method to improve its properties, especially its microscale ductility. Now that many works have proved that Ti_3SiC_2 or Ti_3AlC_2 can be formed in TiC, the key point is how to realize the controllability of these, including their quantity and distribution. According to previous works [4,5], the formation of Ti_3SiC_2 or Ti_3AlC_2 platelets in TiC is closely related to two steps: the first is the doping and diffusion (relocation) of Si/Al in the lattice, the second is the formation of microtwins or stacking faults. These two steps may influence each other. It has been considered that the doping of Si/Al would induce the formation of microtwins or stacking faults, but there is another possibility, i.e. that microtwins or stacking faults are formed first, and then their formation promotes the doping and segregation of Si/Al and leads to formation of Ti_3SiC_2/Ti_3AlC_2 platelets.

Therefore, to clarify the relationship between the microtwins or stacking faults (SFs) and the doping of Si, their interaction is studied in this work, and we think that this study will be helpful in realizing controllable formation of $M_{n+1}AX_n$ platelets in TiC.

II. Calculations Methods

The calculations are based on the density-functional theory and performed with CASTEP. The generalized gradient approximation (GGA) of Perdew and Wang (PW91) is utilized for energy calculation. The TiC (111) plane with a slab of 8.5-layers and 20 Å of vacuum region in the z-direction is used as shown in Fig. 1a. Ti-terminated (111) is only considered in this work owing to the unstability of C-terminated (111) surface as reported in Johansson's work [8]. The plane-wave cut-off energy of 350 eV is employed in the calculations, which can assure tolerances of energy and displacement convergence of 5.0×10^{-6}eV/atom and 5.0×10^{-4} Å, respectively. And the grids of K-points were sampled based on $9 \times 5 \times 1$.

The formation energy of the doping of Si is first calculated with Equation (1):

$$E_f = \frac{E_{tot}^{nSi} - E_{tot} - nE_{Si}}{n} \quad (1)$$

where n is the number of Si atoms, E_{tot}^{nSi} is the total energy of the system with n Si atoms, E_{tot} is the total energy of TiC_x, and E_{Si} is the point potential energy of the Si atom.

* Corresponding author: 52452061@ncepu.edu.cn

While the stacking fault energy is also calculated and defined as,

$$SFE = \frac{E_{SF} - E_{ideal}}{A} \quad (2)$$

where E_{SF} is the energy of the configuration with a SF, E_{ideal} is the energy of the configuration with the ideal sequence, A is the interface area which the SF extends in the (111) plane.

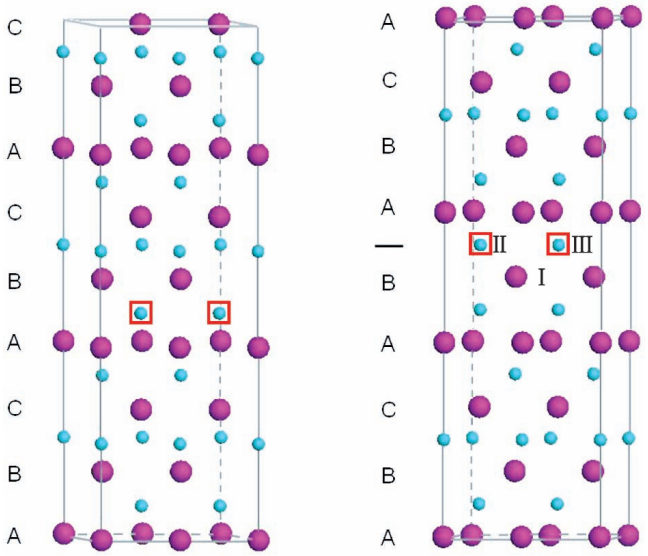

Fig. 1: Configurations used in this study. The purple and blue balls represent Ti and C, respectively. The positions of carbon vacancies are marked by the red boxes. (a) TiC(111) with the ideal sequence; (b) TiC(111) with the stacking sequence.

In addition, the linear synchronous transit (LST) optimization method is also used to study the diffusion of Si. A series of single-point energy calculations are performed on a set of linearly interpolated structures between an initial and a final state in LST optimization. The maximum energy structure along this path provides a first estimate of the transition state structure. Then, an energy minimization in directions conjugate to the reaction pathway is performed [9], which yields a structure closer to the true transition state and can be used to determine the energy barrier of the diffusion process.

III. Results and Discussions

The doping of Si in TiC crystal lattice is first investigated. Two possible positions for the doped Si in perfect TiC are considered, the first one is the Ti site and the second is the carbon site. The formation energy of the doping of Si is calculated with Equation (1) and the result is shown in Table 1. It can be seen that the formation energy of the doped Si in the Ti site is lower than that in the carbon site, indicating that Si prefers to locate in the Ti site. But it is also found that even the formation energy in the Ti site at 6.04 eV/atom is very high, demonstrating that the doping of Si in perfect TiC is very difficult. These results are in accordance with previous works, which also found that the difficult doping of Si/Al in perfect TiC crystal lattice and they confirmed that the doping of Si/Al in TiC is associated with lattice defects such as vacancies, stacking faults [10]. This is also matched with the character of the true TiC crystal lattice. It is known that TiC is never experimentally found to be fully stoichiometric, but contains many carbon vacancies while keeping the same crystallographic structure and up to one-half of carbon lattice sites can be vacant [11–14]. So, studying the doping of Si in TiC_x that contains carbon vacancies would be more meaningful. Moreover, this work mainly investigates the interaction of SFs and the doping of Si as mentioned above, while the SFs are also closely related to the carbon vacancies and the SFs can be much more easily formed in TiC_x with an amount of carbon vacancies [15–17], especially in TiC_x with ordered carbon vacancies which would result in the emptying of some {111} carbon planes [18,19]. Therefore, a special configuration containing the ordered carbon vacancies is used to study the doping of Si in non-stoichiometric TiC_x and the positions of the vacancies are marked by red boxes in Fig. 1a.

Table 1: Formation energies for the doping of Si in TiC.

Configurations	E_f (eV/atom)		
	Ti sites	C sites	Vacancies
Perfect TiC	6.04	6.21	–
TiC with ordered C vacancies	3.43	–	-6.23
TiC with SFs	5.69	6.31	–
TiC with SFs and C vacancies	3.70	–	-5.71

Two possible positions for the doped Si are considered. The first is the Ti site next to the carbon vacancy, and the second is the carbon vacancy site. The formation energies are also shown in Table 1. It can be seen that it is 3.43 eV/atom for Si in the Ti site. Although it is still high, it is much lower than that in perfect TiC. It is noticed that the formation energy for doping of Si in the carbon vacancy is -6.23 eV/atom, which indicates that the doping of Si in ordered carbon vacancies is thermally favorable. This may be due to the weak bonding between the Ti-Ti layers in TiC_x and the doping of Si results in the forming of the stronger Ti-Si bonds.

The doping of Si in TiC with SFs is then examined and the TiC(111) with SFs but without vacancies is shown in Fig. 1b. The doping of Si in Ti sites and C sites around SF layers are firstly considered and the formation energies are shown in Table 1. Like that in TiC without SFs, the doping of Si in Ti site is also more favorable than that in C site. And the formation energy in Ti site is 5.69 eV/atom, which is lower than in TiC without SFs. This indicates that SFs are beneficial for the doping of Si. For TiC_x with both SFs and ordered carbon vacancies, the positions of which are also marked by red boxes in Fig. 1b, it is found from Table 1 that the formation energies for doping of Si in both the Ti site and carbon vacancy are much smaller

than that in TiC without vacancies and the doping of Si in carbon vacancies are also thermally favorable, but they are larger than that in TiC_x with ordered carbon vacancies while without SFs. According to our previous work [15], when containing ordered carbon vacancies, TiC_x with SFs is more stable than that without SFs, which means that the Ti-Ti bonds in TiC_x with both SFs and ordered carbon vacancies are stronger than those in TiC_x without SFs. Therefore, it is reasonable for the more difficult formation of Ti-Si bonds which is associated with the break of Ti-Ti bonds.

It is known that the density of states (DOS) is an important quantity for understanding the bonding in a compound. Thus, in order to further clarify the influence of the doping of Si, the DOS and PDOS (partial density of states) of TiC (111) are then examined and the results are shown in Fig. 2. It can be seen from Fig. 2a that the DOS of TiC(111) consists of three parts. The peak between -12 to -9 eV is dominated by C-2s states, which contributes little to the bonding of TiC [20]. The peaks just below the Fermi level (E_F) contains strongly hybridized C-2p and Ti-3d states and the major component is C-2p bands, demonstrating the formation of Ti-C covalent bonds [21]. In addition, the peak which is mainly composed of 3d orbitals of Ti and some of the C-2p orbitals at the E_F indicates the obviously metallic characteristic of TiC(111). When the ordered carbon vacancies are introduced, the peaks are changed obviously, as shown in Fig. 2c. It is found that a small peak below the E_F appears. This peak is attributed to the Ti-3d and Ti-3p states, proving the formation of Ti-Ti bonds. At the same time, in comparison with that in Fig. 2a, the C-2p and Ti-3d hybridized peak is more localized, demonstrating the degradation of Ti-C covalent bonds. After the doping of Si, the peaks corresponding to the Ti-Ti bonds disappear owing to the p-d hybridization of Ti and Si atoms, as shown in Fig. 2e. For TiC with SFs as shown in Fig. 2b, the peak corresponding to the hybridization of C-2p and Ti-3d is narrower than that in Fig. 2a while the peak at the E_F, which is dominated by Ti-3d states, is much wider. These results confirm that the formation of SFs in TiC will weaken the covalent bonding of Ti-C while enhancing the metallic bonding, which may be helpful for improving the conductivity of TiC. This will be discussed in our future work. When TiC contains both SFs and ordered carbon vacancies, the peak at E_F is much wider, as shown in Fig. 2d. After the doping of Si in vacancy sites, the peak that is attributed to the d-p hybridization of Ti and C/Si is the widest among Fig. 2b, d and f, indicating the stronger covalent bonding.

The influence of doped Si on the formation of SFs is then examined. The stacking fault energy (SFE) of TiC without carbon vacancies is firstly calculated with Equation (2) and the results are shown in Table 2. It is found that when a Si atom is doped in a Ti site, the SFE is about 1.026 J/m^2, which is lower than that in perfect TiC but higher than that in TiC with a carbon vacancy. This indicates that the doped Si is helpful for the formation of SFs in TiC, but its efficiency is much weaker than the carbon vacancies. In order to further confirm this conclusion, the simultaneous effect of carbon vacancies and doped Si on SFE is also investigated. The configurations with the doped Si located in position I or II as shown in Fig. 1b, and two doped Si located in positions II and III are all considered. It can be seen from Table 3 that when Si is combined with one carbon vacancy (located in position II), the SFE is 0.432 J/m^2, and when Si atoms are combined with all the carbon vacancies that can be identified as the formation of Ti_3SiC_2 platelet, the SFE further increases to 0.735 J/m^2. However, when the doped Si is located in the Ti site (located in position I), the SFE is reduced to 0.186 J/m^2. But it is still higher than that in TiC with ordered carbon vacancies only. These results further confirm that the doped Si can induce the formation of SFs, but its efficiency is weaker than the carbon vacancies.

Table 2: Stacking fault energy (SFE) (J/m^2) of TiC.

Configurations	Perfect TiC crystal	TiC with a carbon vacancy	TiC with a Si atom in different sites	
			in the Ti site	in the C sites
SFE	1.378 [14]	0.838 [15]	1.026	1.481

Table 3: The simultaneous effect of carbon vacancies and doped Si on SFE (J/m^2).

Configurations	TiC with ordered C vacancies	TiC with doped Si around carbon vacancies		
		Position I	Position II	Position II and III
SFE	-0.081 [15]	0.186	0.432	0.735

According to the above results, it can be concluded that the SFs and doping of Si in TiC are influenced by each other. The formation of SFs is favorable for the doping of Si, but this effect is limited, especially in TiC with carbon vacancies. The doped Si can reduce the SFE; however, its efficiency is much weaker than the carbon vacancies. It is noticed that both of them are closely related to the carbon vacancies. The existence of carbon vacancies is essential for the formation of SFs, while it would also be attributed to the doping of Si. Therefore, it is considered that carbon vacancies in TiC firstly induce the SFs and the doping of Si, then the doped Si and carbon vacancies tend to segregate in the SFs layers and lastly evolve to Ti_3SiC_2 as found in Refs. [4, 5]. This process can be further supported by the easier diffusion of the carbon vacancies, as determined in our previous work [14], and Si in SFs layers as shown in Fig. 3. The energy barrier for diffusion of doped Si in SFs layers which means the migration of Si from the original position to the adjacent carbon vacancy is only about 0.11 eV, as shown in Fig. 3a, while it is 0.74 eV in the ideal sequence layers.

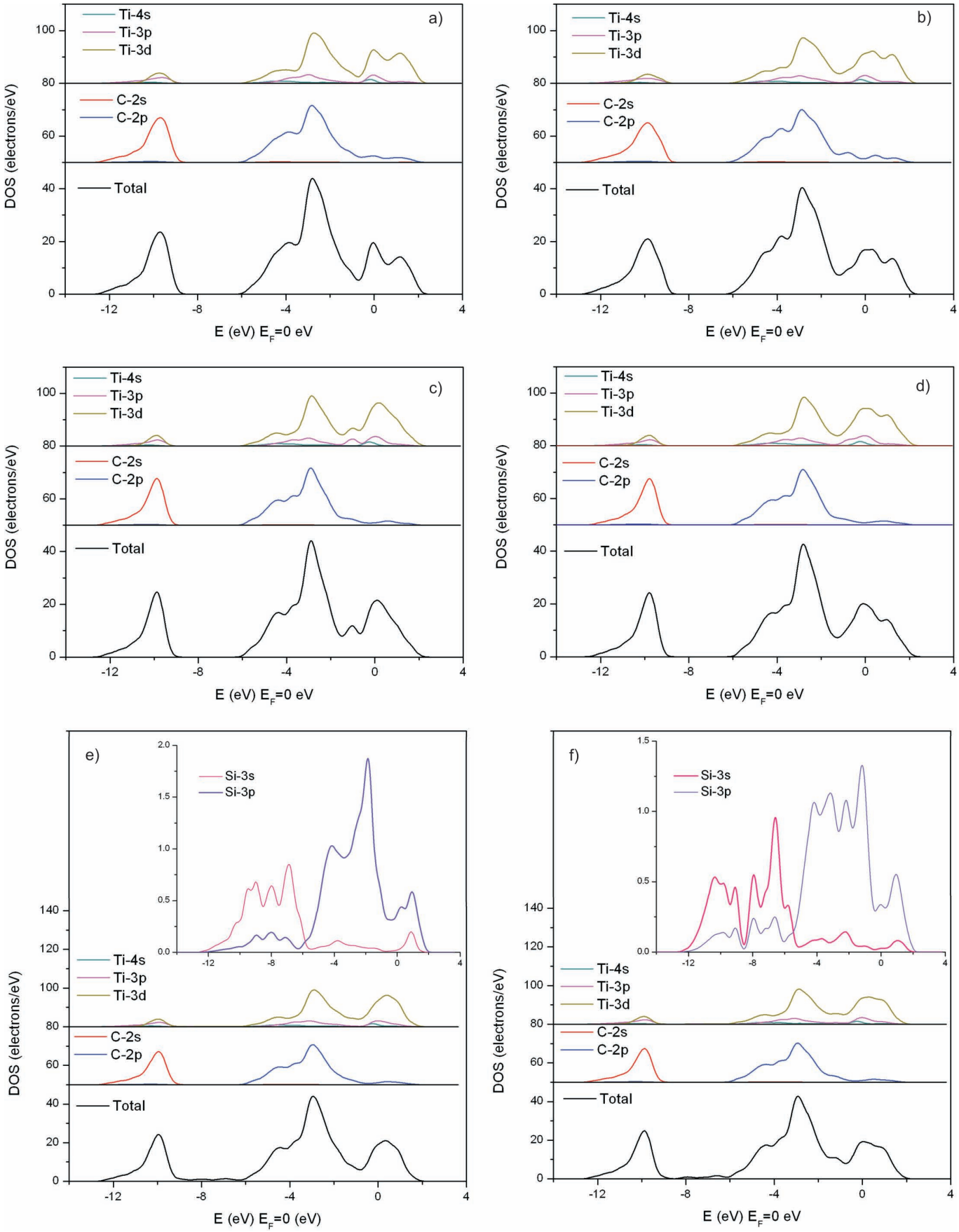

Fig. 2: DOS and PDOS for TiC (111) a) TiC(111) with ideal sequence, c) with carbon vacancies, and e) with doped Si atoms; b) TiC(111) with the stacking sequence, d) with carbon vacancies, and f) with doped Si atoms.

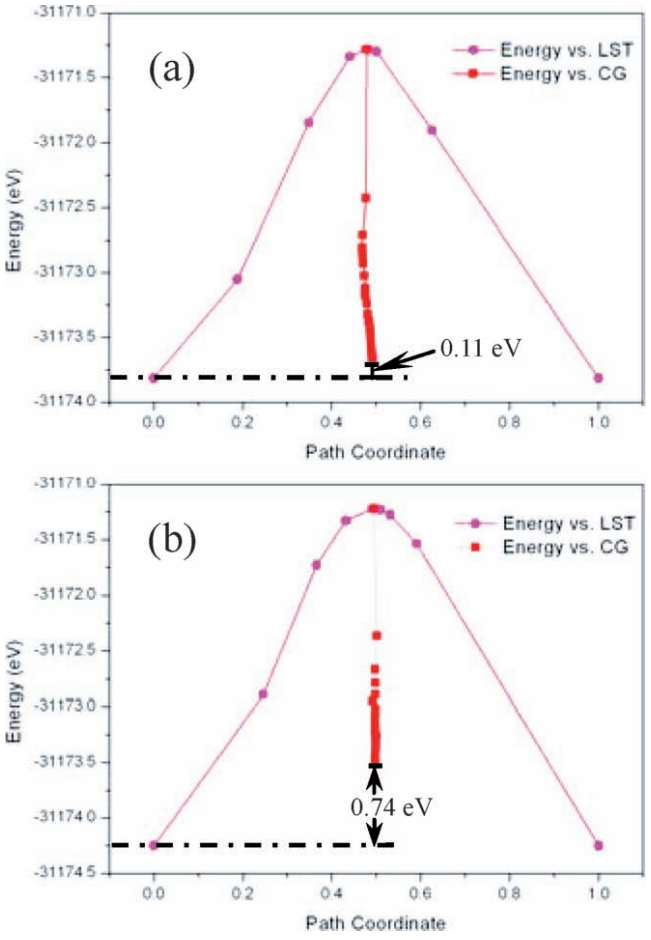

Fig. 3: The calculated diffusion energy profile for doped Si (a) diffusion in the SF layers of TiC(111); (b) diffusion in the ideal sequence layers.

IV. Conclusions

The interaction of stacking faults and the doping of Si in TiC has been studied in this work. It is found that the SFs and doping of Si are influenced by each other. The formation of SFs is favorable for the doping of Si, but this effect is limited. The doped Si can reduce the SFE; however, its efficiency is much weaker than the carbon vacancies. It is noticed that both are closely related to the carbon vacancies. It is considered that the carbon vacancies are the key for both the SFs and doping of Si and simultaneously promote the formation of SFs and the doping of Si, then the doped Si and carbon vacancies tend to segregate in the SFs layers. And the segregation process can be enhanced by the SFs owing to their much easier diffusion in SFs layers.

Acknowledgments

This work was supported by the National Nature Science Foundation of China (No. 51301068), the Natural Science Foundation of Hebei Province (No. E2014502003) and the Fundamental Research Funds for the Central Universities (No. 2016MS112).

References

1 Miriyev, A., Sinder, M., Frage, N.: Thermal stability and growth kinetics of the interfacial TiC layer in the ti alloy/carbon steel system, *Acta Mater.,* **75**, 348 – 355, (2014).

2 Zhang, Y., Xiao. G., Xu, C., Yi, M., Meng, X.: Anisotropic fracture toughness and microstructure of graphene-reinforced TiC/Si_3N_4 composite, *J. Ceram. Sci. Tech.,* **4**, 323 – 327, (2016).

3 Zhou, M.Y., Rodrigo, P.D.D., Wang, X.J., Hu, J.B., Dong, S.M., Cheng, Y.B.: A novel approach for preparation of dense TiC-SiC nanocomposites by sol-gel infiltration and spark plasma sintering, *J. Eur. Ceram. Soc.,* **34**, 1949 – 1954, (2014).

4 Yu, R., Zhan, Q., He, L.L., Zhou, Y.C., Ye, H.Q.: Si-induced twinning of TiC and formation of Ti_3SiC_2 platelets, *Acta Mater.,* **50**, 4127 – 4135, (2002).

5 Yu, R., He, L.L., Ye, H.Q.: Effects of Si and Al on twin boundary energy of TiC, *Acta Mater.,* **51**, 2477 – 2484, (2003).

6 Zhou, C.L., Ngai, T.W.L., Lu, L., Li, Y.Y.: Fabrication and characterization of pure porous Ti_3SiC_2 with controlled porosity and pore features, *Mater. Lett.,* **131**, 280 – 283, (2014).

7 Istomin, P., Nadutkin, A., Grass, V.: Fabrication of Ti_3SiC_2-based ceramic matrix composites by a powder-free SHS technique, *Ceram. Int.*, **39**, 3663 – 3667, (2013).

8 Johansson, L.I.: Electronic and structural properties of transition-metal carbide and nitride surfaces, *Surf. Sci. Rep.*, **21**,177 – 250, (1995).

9 Govind, N., Petersen, M., Fitzgerald, G., King-Smith, D., Andzelm, J.: A generalized synchronous transit method for transition state location, *Comput. Mater. Sci.*, **28**, 250 – 258, (2003).

10 Music, D., Riley, D.P., Schneider, J.M.: Energetics of point defects in TiC, *J. Eur. Ceram. Soc.,* **29**, 773 – 777, (2009).

11 Zhang, P., Nie, J.F., Gao, T., Wang, T., Liu, X.F.: Influence of nitrogen on the synthesis and nucleation ability of TiC_x in Al-Ti-C master alloy, *J. Alloy. Compd.* **601**, 267 – 273, (2014).

12 Tsetseris, L., Pantelides, S.T.: Vacancies, interstitials and their complexes in titanium carbide, *Acta Mater.,* **56**, 2864 – 2871, (2008).

13 Guemmaz, M., Mosser, A., Parlebasb, J.C.: Electronic changes induced by vacancies on spectral and elastic properties of titanium carbides and nitrides, *J. Electron Spectrosc.,* **107**, 91 – 101, (2000).

14 Hugosson, H.W., Korzhavyi, P., Jansson, U., Johansson, B., Eriksson, O.: Phase stabilities and structural relaxations in substoichiometric TiC_{1-x}, *Phys. Rev. B*, **63**, 165116 – 165123, (2001).

15 Ding, H.M., Fan, X.L., Chu, K.Y., Zhang, X.C., Liu, X.F.: The influence of carbon vacancies on the stacking fault energy of TiC, *J. Eur. Ceram. Soc.,* **34**, 1893 – 1897, (2014).

16 Li, X.X., Xiang, J.Y., Hu, W.T.: {111} twinning structure and interfacial energy in nonstoichiometric TiC_x with ordered carbon vacancies, *Mater. Charac.,* **90**, 94 – 98, (2014).

17 Tsurekawa, S., Yoshinaga, H.: Dislocation dissociation in titanium carbide crystal, *J. Japan Inst. Metals*, **58**, 390 – 396, (1994).

18 Bursik, J.: Ordering of substoichiometric δ-TiC_x phase in Ti-V-C alloys, *Phys. Stat. Sol. A*, **174**, 327 – 335, (1999).

19 Barsoum, M.W.: The $M_{N+1}AX_N$ phases: A new class of solids, *Prog. Solid State Chem.,* **28**, 201 – 281, (2000).

20 Price, D.L., Cooper, B.R.: Total energies and bonding for crystallographic structures in titanium-carbon and tungsten-carbon systems, *Phys. Rev. B*, **39**, 4945 – 4957, (1989).

21 Dridi, Z., Bouhafs, B., Ruterana, P., Aourag, H.: First-principles calculations of vacancy effects on structural and electronic properties of TiC_x and TiN_x, *J. Phys.: Condens. Matter,* **14**, 10237 – 10249, (2002).